Original Article

Cytogenet Genome Res 121:1–6 (2008)
DOI: 10.1159/000124373

Cytogenetic and Genome Research

Sequence based high resolution chromosomal CGH

A. Kowalska[a] B. Brunner[a] E. Bozsaky[a] Q.-R. Chen[b] C. Stock[a] T. Lörch[c] J. Khan[b] P.F. Ambros[a]

[a]CCRI, Children's Cancer Research Institute, St. Anna Kinderkrebsforschung, Vienna (Austria)
[b]Oncogenomics Section, Pediatric Oncology Branch, National Cancer Institute, National Institutes of Health, Bethesda, MD (USA); [c]MetaSystems, Altlussheim (Germany)

Accepted in revised form for publication by M. Schmid, 10 December 2007.

Abstract. We aimed to directly align a chromosomal CGH (cCGH) pattern with the gene mapping data by taking advantage of the clustering of the GGCC motif at certain positions in the human genome. The alignment of chromosomal with sequence data was achieved by superimposition of (i) the fluorescence intensity of the sequence specific fluorochrome, Chromomycin A3 (CMA3), (ii) the cCGH fluorescence intensity profile of individual chromosomes and (iii) the GGCC density profile extracted from the Ensembl genome sequence database. The superimposition of these three pieces of information allowed us to precisely localize regions of amplification in the neuroblastoma cell line STA-NB-15. Two prominent cCGH peaks were noted, one at 2p24.3, the position 15.4 mega base (Mb), and the other at 2p23.2, 29.51 Mb. FISH and high resolution array CGH (aCGH) experiments disclosed an amplification of *MYCN* (16 Mb) and *ALK* (29.2–29.9 Mb), thus confirming the cCGH data. The combined visualization of sequence information and cCGH data drastically improves the resolution of the method to less than 2 Mb.

Cancer initiation and progression is thought to be driven by chromosome rearrangements which frequently result in genomic imbalances. Thus, the knowledge of genomic alterations contributing to tumor pathogenesis enhances our understanding of this process and, what is of great importance, provides new diagnostic and prognostic tools. Conventional cytogenetic methods are based on chromosome banding with various stains followed by identification of individual chromosomes and detection of chromosomal alterations. However, karyotyping frequently raises difficulties because the quality of metaphase spreads is often inadequate or the cells exhaust their proliferative activity as is, for instance, the case in differentiated or senescent cells. This limitation was circumvented by a molecular cytogenetic method, comparative genomic hybridization (Kallioniemi A et al., 1992; Kallioniemi OP et al., 1994). cCGH has already made a significant impact on cancer cytogenetics. It is one of the more widely used methods for detecting large-scale gains or losses of genetic material in tumors as it enables genome-wide screening for imbalances in a single hybridization experiment (Kallioniemi A et al., 1994; Lichter et al., 1995, 2000; Stock et al., 2000; Wang, 2002; Garnis et al., 2004). cCGH involves competitive hybridization of differentially labeled (e.g. red and green) tumor and normal whole genomic DNAs in equal amounts to normal metaphase spreads. Accordingly, the relative amount of tumor and reference DNA bound at a given chromosomal locus depends on the relative abundance of DNA copy number in the two samples. These differences can be quantified by measurement of the green-to-red fluorescence intensity ratio. Regions of lost or gained DNA sequences, i.e. deletions, duplications, or amplifications appear as changes in the fluorescence intensities of the two fluorochromes along the target chromosomes.

This work was supported by St. Anna Kinderkrebsforschung.

Request reprints from Peter F. Ambros
CCRI, St. Anna Kinderkrebsforschung
Kinderspitalgasse 6, AT–1090 Vienna (Austria)
telephone: +43 1 40470 4110; fax: +43 1 40470 7150
e-mail: peter.ambros@ccri.at

1424–8581/08/1211–0001$24.50/0

Accessible online at:
www.karger.com/cgr

Although cCGH provides a fluorescence profile of the entire genome, the method has so far been restricted by a relatively low sensitivity mainly due to the fact that the results are averages from profiles of a number of inconsistently aligned chromosomes. Thus, it has been difficult to assign gains and losses to the specific chromosomal positions. According to simulation experiments, single copy deletions of 2 Mb should be detectable (Piper et al., 1995). However, cCGH experiments have shown that single copy deletions can be reliably detected by fixed thresholds if they are in the range of 10–20 Mb (Kallioniemi A et al., 1992; Kallioniemi OP et al., 1994; Bentz et al., 1998; Pinkel et al., 1998). The second and even more striking flaw of the classical cCGH technique is the lack of any direct linkage of the cCGH fluorescence pattern with the gene map data. Thus, it has so far not been feasible to precisely ascertain which genomic loci are anchored by the gained, amplified or lost chromosomal regions. One alternative is the application of CGH to target DNA sequences on microarrays (aCGH) which leads to the increase in resolution (determined by the number of probes spotted on the tracer) and allows a direct identification of the gained or lost sequences (Pinkel et al., 1998; Lichter et al., 2000; Chen et al., 2004, 2005). However, to analyze aCGH data, special equipment is required which is not necessarily available in standard laboratories. Thus, we attempt to devise an appropriate method to link the fluorescence profile of chromosomal copy number alterations detected with cCGH with the genome sequence data and establish an internal anchoring system that facilitates profile alignment and thus increases the resolution of cCGH. Using the sequence specific fluorochrome Chromomycin A3 (CMA3), which highlights GGCC specific chromosomal regions (Schweizer, 1976; Schweizer and Ambros, 1994; Hou et al., 2004), the chromosome banding information, i.e. CMA3 fluorescence intensity curve reflecting the alternations of GGCC density along the chromosome, can be directly 'translated' into the genome sequence information. This so-called sequence banding is superimposed on the GGCC motif density profile extracted from the Ensembl genome sequence database (http://www.ensembl.org). Such rapid and direct assignment of chromosomal bands with the gene mapping data makes it possible to define every chromosomal locus not only in cytobands but also in mega base pairs (Mb). To achieve this goal a software termed ISIS External Profiles Function and the Warp tool were developed (Kowalska et al., 2007). Here, we addressed the question whether the simultaneous visualization of cCGH fluorescence intensities and sequence banding results in a more precise interpretation of cCGH results. These results were validated by FISH and high resolution aCGH.

Materials and methods

Chromosomal comparative genomic hybridization (cCGH)

We cohybridized differentially labeled DNAs derived from a neuroblastoma cell line STA-NB-15 (Narath et al., 2007) and leukocytes (the reference sample) to the target metaphase spreads. DNAs were prepared according to standard protocol, including digestion in Lysis buffer Mix (containing Proteinase K (20 mg/ml) and 20% SDS) and 6 M NaCl treatment, followed by precipitation and dissolving in 1× TE buffer (pH 8). cCGH procedure was followed as described previously (Kallioniemi A et al., 1992; Kallioniemi OP et al., 1993; Stock et al., 2000). Briefly, STA-NB-15 and reference DNA were differentially labeled with DEA Coumarin 5-dUTP (1 mM) (New England Nuclear) and Alexa Fluor-568-dUTP (1 mM) (Molecular Probes) by nick-translation labeling procedure according to the standard protocol. Then the samples were cohybridized to normal metaphase spreads in the presence of human Cot-1 DNA (Roche, Mannheim, Germany). Metaphase chromosome preparations were made from normal human peripheral lymphocyte cultures harvested by standard cytogenetic methods. The modification we have introduced to the standard cCGH protocol was that target chromosomes to which differentially labeled DNAs were hybridized were stained with CMA3 and all three fluorescence intensity profiles were acquired simultaneously.

Chromomycin A3 staining

To visualize CMA3 banding pattern on the chromosomes Chromomycin A3 (CMA3), Distamycin A (DA) and DAPI staining (CDD triple staining) was performed according to the standard protocol (Schweizer, 1976; Schweizer and Ambros, 1994). By using distamycin/DAPI as counterstains the contrast of the CMA3 bands is increased (Schweizer, 1981). CMA3 solution (0.5 mg/ml, in McIlvane's buffer (pH 7) diluted 1:1 with water, containing 0.005 volume 1 M $MgCl_2$) was applied on the slides which were then covered with a plastic cover slip and incubated overnight at room temperature in the dark. After that, the slides were rinsed in deionized water, blown dry and distamycin solution (1 mg/ml, in McIlvane's buffer (pH 7)) was applied for 10 min. This was followed by rinsing in deionized water and staining with DAPI solution (2 mg/ml in McIlvane's buffer (pH 7) diluted 1:1000 with PBS; 15 min). The slides were mounted in an antifade solution (87% Glycerol:McIlvane's (pH 7) 1:1, plus 250 μl 1 M $MgCl_2$) mixed with a Vectashield mounting medium for fluorescence (Vector Laboratories) in 1:1 ratio and incubated at least 3 d at 37°C. The inclusion of Mg^{2+} as well as the aging of slides for at least 3 d is crucial to obtain a stable CMA3 fluorescence. In order to analyze the fluorescence intensities of all three pieces of information – CMA3, test DNA and reference DNA – the choice of adequate combination of fluorescent dyes is of great importance. CMA3 was used instead of DAPI banding which has frequently been employed for chromosome identification. We considered CMA3 peaks superior to reverse DAPI peaks which appear less well defined especially in the telomeric regions. The External Profiles Function and the Warp tool were applied as described elsewhere (Kowalska et al., 2007).

Oligonucleotide array CGH (aCGH)

For the oligonucleotide array CGH experiment, array construction, DNA labeling, hybridization, and washing were performed as described in detail by Selzer et al. (2005). Briefly, the tiling-path CGH arrays were designed for whole-genome analysis with up to 385,000 oligonucleotides from unique sequence regions that are of variable length to achieve a melting temperature of 76°C. Genomic DNA was randomly fragmented by sonication to a size range of 500–2,000 bp. Control (reference) male human genomic DNA samples (Promega, Madison, WI) were used in hybridization. Each DNA sample is directly labeled by random primer extension labeling (Cy3 for tumor sample and Cy5 for the reference DNA). The Cy3 labeled tumor sample and Cy5 labeled reference sample were combined and applied for hybridization as described (Selzer et al., 2005). Data were extracted from scanned images using NimbleScan 2.0 extraction software (NimbleGen Systems, Inc.).

Fig. 1. Assignment of cCGH profile to the genome sequence information using External Profiles Function and Warp tool. **(A)** Definition of the longitudinal axis (white line) of normal human chromosome 2 after hybridization of differentially labeled STA-NB-15 and reference DNAs and simultaneous staining with CMA3. The white line indicates the track of the measured fluorescence intensity. The cCGH fluorescence intensity ratio profile and the CMA3 fluorescence profile are visualized as intensity curves in **B**, the white curve in the lower part of the picture corresponds to the ratio profile of STA-NB-15 to the reference fluorescence; the blue curve illustrates GGCC motif frequency based on the CMA3 fluorescence intensity; the white curve in the upper part of the picture represents the GGCC density according to Ensembl databank; yellow lines denote linkage of landmarks. Pter is defined as the first landmark at 0 bp (on the left side), qter as the last position (on the right side) and the centromere as GC-poor domain (low fluorescence intensity in submedial region). Most prominent peaks and valleys of GGCC density are set as secondary landmarks. **(C)** 'Warped' chromosome 2 after combined cCGH and CMA3 fluorescence and superimposing of the chromosomal sequence information to the database sequence information. The cell line used for cCGH analysis displays two peaks on 15.16 Mb (a) and 29.11 Mb (b).

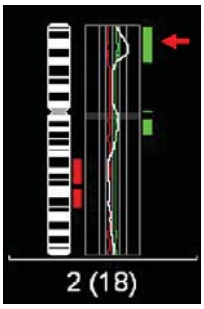

Fig. 2. 'Classical' cCGH profile of STA-NB-15 cell line showing a gain (amplification) of 2pter–p22 region (green bar indicated by arrow), with only one peak at 2p22 (peak of the white curve).

Results

The application of the External Profiles Function and the Warp tool to chromosomes displaying both the cCGH fluorescence pattern and the GGCC distribution highlighted by the CMA3 staining, is shown in Fig. 1. Chromosome 2 (Fig. 1A) was chosen to demonstrate the entire fluorescence intensity information, i.e. CMA3 profile and the STA-NB-15-to-reference ratio profile. The fluorescence intensity ratio curve and CMA3 curve obtained by interactive definition of the longitudinal axis of the chromosome are given in the lower part of Fig. 1B: the blue curve represents the CMA3 fluorescence intensity reflecting GGCC motif frequency along the chromosome axis, the white curve illustrates the ratio between fluorescence intensities of DEAC labeled 'test' DNA (neuroblastoma cell line) and red labeled 'reference' DNA (leukocytes). The white curve in the upper part of Fig. 1B delineates the GGCC sequence density extracted from Ensembl database. With the ISIS External Profiles Function telomeres, centromeres and positive and negative CMA3 fluorescence peaks (blue curve in the lower part of Fig. 1B) were aligned to the corresponding regions in the Ensembl database (white curve in the upper part) by drawing yellow lines (so-called landmarks) between both curves. After linking the landmarks between the two profiles, the Warp tool enables exact localization of CGH ratio profiles in cytoband and Mb positions (Fig. 1C). The 'warped' chromosome 2 displaying two prominent cCGH peaks of the ratio profile on 2p, with Mb and cytoband positions, is illustrated in Fig. 1C. Employing External Profiles Function and the Warp tool the distal peak (marked with 'a' in Fig. 1C) was localized at 15.16 Mb, 2p24.3. The more proximal peak position ('b' in Fig. 1C) was determined at 29.11 Mb, 2p23.2. After analysis of 20 different chromosomes 2 the mean result of the position measurements was 15.4 and 29.51 Mb. This proves the enhancement of the cCGH resolution using the Warp tool in comparison with the 'classical' cCGH profile showing only one single peak at 2pter→2p22 (Fig. 2).

The aCGH data (Fig. 3) of the chosen neuroblastoma cell line disclosed coamplification of two distinct loci corresponding to *MYCN* and *ALK*. According to the Ensembl database, the *MYCN* gene is located at the position 16 Mb (2p24.3); the position reported for *ALK* is 29.2–29.9 Mb, 2p23.2→p23.1. Thus, the Warp tool findings were in line with the aCGH data. Mean difference between the *MYCN* and

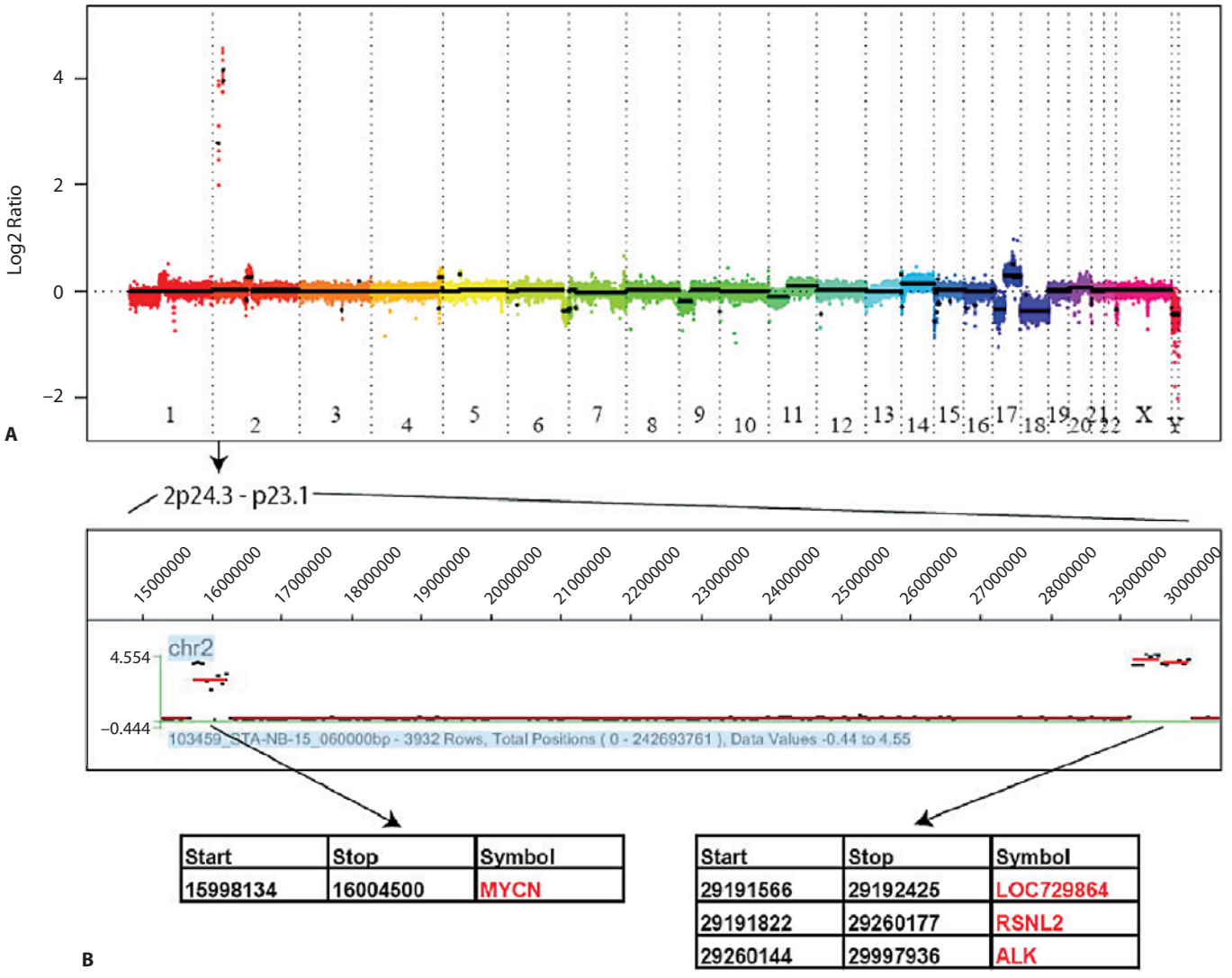

Fig. 3. Whole genome aCGH analysis on STA-NB-15. Log2 ratio on the vertical axis is plotted against genome position (HG18) on the horizontal axis. Each point represents the average fluorescence intensity of the oligos contained within a 60-kb window, with the midpoint of the window used as the genome position. **(A)** The entire genome is shown on the top panel. **(B)** The region of 2p24.3→p23.1 is shown with two amplicons: 1. amplicon contains *MYCN*; 2. amplicon contains *LOC729864*, *RSNL2* and *ALK*.

ALK positions measured with External Profiles Function and Warp tool and the gene positions given in Ensembl database was 1.5 Mb (range: 0.04–4.10 Mb). The median value was –0.41 Mb in case of *MYCN* and –0.68 Mb in case of *ALK*. In order to reconfirm the correspondence of mapped cCGH peaks to the localization of *MYCN* and *ALK* genes we labeled RP11–480N14 (*MYCN*) and RP11–328L16 (*ALK*) probes in red, and sequentially hybridized them to the slides on which cCGH and 'warping' were performed. Previously acquired metaphases were relocated with the help of saved slide coordinates. The FISH image of the identical metaphase was recaptured in the red channel of existing cCGH image followed by merging of both sets of information. It resulted in co-localization of the high fluorescence intensity cCGH signals reflecting amplification at *MYCN* and *ALK* loci with FISH signals of *MYCN* and *ALK* probes (data not shown).

Discussion

High resolution aCGH data confirmed the amplification of *MYCN* and *ALK* genes visualized in the neuroblastoma cell line with classical chromosomal CGH. The cCGH technique itself lacks high sensitivity and gene specificity – the resolution of 10–20 Mb is far below that of aCGH. However, application of the External Profiles Function and the Warp tool tremendously improves cCGH accuracy. The data presented here imply that combination of chromosomal CGH pattern with the CMA3 banding, so-called sequence banding, and the subsequent analysis with the Warp tool considerably elevates the cCGH resolution to less than 2 Mb and provides a direct assignment of cCGH profiles to gene map data. Therefore, the cCGH could be directly compared with aCGH resulting in highly concordant data.

Chromosomal CGH has several advantages over the approaches which target microarrays. The technique is relatively simple, rapid and widely accessible. Most likely, one of the obstacles researchers face using microarrays are storage and analysis of vast quantities of data. In comparison, the amount and complexity of the data generated by cCGH is less and, what is of great importance, the analysis is independent of selecting sequences for interrogation (the set of genes, clones, oligos etc. on the array). cCGH, in contrast to aCGH, provides a comprehensive view of all regions in the genome including also those sequences which are usually omitted on the arrays (e.g. repetitive sequences).

Kirchhoff et al. (1998, 1999, 2001) increased sensitivity and specificity of cCGH to 3 Mb by using standard reference intervals. The elevated resolution was solely associated with the detection criteria and not with the preparation of cCGH slides and application of the diagnostic threshold. The resolution of less than 2 Mb, which was achieved by the simultaneous demonstration of the cCGH and sequence banding information, indicates that our approach has the capacity to reach the theoretical sensitivity limit proposed by Piper and coworkers (Piper et al., 1995).

The External Profiles Function and the Warp tool utilize individual chromosomes. Therefore, for an overall genome-wide screening for gains, losses or amplification in the test samples it is advised to perform classical chromosomal CGH which provides an average result from a number of metaphases. However, cCGH can also be used to analyze individual chromosomes in combination with the Warp tool, i.e. for assigning the fluorescent peaks of interest to the Mb positions and thus to the gene map data.

Since telomeric and centromeric regions have never been completely sequenced, they have an assumed standard size in the different databases (Ensembl, NCBI) although in fact they are polymorphic in length between donors (Aviv et al., 2003). Such intra- and interindividual discordances in telomere and centromere length relative to the arbitrarily assumed sequence data may elevate heterogeneity and imprecision in defining the position of a chromosomal locus. However, as paracentromeric heterochromatin can easily be identified using CMA3 staining these regions do not cause any mapping problems (for further details see Kowalska et al., 2007). Additionally, since telomere repeats span only 4–14 kb (de Lange et al., 1990; Knight and Flint, 2000; Lin and Yan, 2005) such length variability might be neglected, as it is below the sensitivity of our method. On the other side, subtelomeric repeat DNA regions can stretch from 10 to 500 kb (Riethman et al., 2005; Ambrosini et al., 2007) and this variation in length may lead to differences between individual chromosomes in assignment of those regions to the static sequence information. Furthermore, the GGCC densities given in the sequence data base are characterized by a drastic increase (pter) or decrease (qter) of the base frequency. In contrast, the CMA3 fluorescence intensity reflecting the GGCC density of the chromosome does not abruptly increase or decrease. However, a gradual increase or decrease of the fluorescence intensity can be noticed at the chromosomal ends. The fact that (i) the chromosomal ends are not well defined and (ii) the subtelomeric sequences are variable in length accounts for a less accurate mapping of subtelomeric or telomeric markers. However, as interchromosomal positive and negative bands can be used as landmarks, virtually all interchromosomal positions can be precisely mapped with our technique (Kowalska et al., 2007).

Accurate alignment of all fluorescence channels of the captured metaphase is an essential requirement to take full advantage of the mapping potential of the Warp tool. Even a slight discordance in the merged pictures may cause an error in the mapping results. Therefore, images composed of different fluorescence channels have to be aligned with great precision.

The simultaneous application of cCGH in combination with chromosome staining using a GGCC specific fluorescent dye enables us to overcome the main drawbacks of cCGH which are a relatively low resolution and the lack of direct linkage of cCGH information with sequence information. Thus, this combined use of sequence banding and cCGH will prove useful to more precisely assign gains, amplifications and losses to genomic positions.

Acknowledgement

We thank Marion Zavadil for proof reading.

References

Ambrosini A, Paul S, Hu S, Riethman H: Human subtelomeric duplicon structure and organization. Genome Biol 8:R151 (2007).

Aviv A, Levy D, Mangel M: Growth, telomere dynamics and successful and unsuccessful human aging. Mech Ageing Dev 124:829–837 (2003).

Bentz M, Plesch A, Stilgenbauer S, Dohner H, Lichter P: Minimal sizes of deletions detected by comparative genomic hybridization. Genes Chromosomes Cancer 21:172–175 (1998).

Chen QR, Bilke S, Wei JS, Whiteford CC, Cenacchi N, et al: cDNA array-CGH profiling identifies genomic alterations specific to stage and MYCN-amplification in neuroblastoma. BMC Genomics 5:70 (2004).

Chen QR, Bilke S, Khan J: High-resolution cDNA microarray-based comparative genomic hybridization analysis in neuroblastoma. Cancer Lett 228:71–81 (2005).

de Lange T, Shiue L, Myers RM, Cox DR, Naylor SL, Killery AM, Varmus HE: Structure and variability of human chromosome ends. Mol Cell Biol 10:518–527 (1990).

Garnis C, Buys TP, Lam WL: Genetic alteration and gene expression modulation during cancer progression. Mol Cancer 3:9 (2004).

Hou MH, Robinson H, Gao YG, Wang AH: Crystal structure of the $[Mg^{2+}$-(chromomycin $A3)_2]$-$d(TTGGCCAA)_2$ complex reveals GGCC binding specificity of the drug dimer chelated by a metal ion. Nucleic Acids Res 32:2214–2222 (2004).

Kallioniemi A, Kallioniemi OP, Sudar D, Rutovitz D, Gray JW, et al: Comparative genomic hybridization for molecular cytogenetic analysis of solid tumors. Science 258:818–821 (1992).

Kallioniemi A, Kallioniemi OP, Piper J, Tanner M, Stokke T, et al: Detection and mapping of amplified DNA sequences in breast cancer by comparative genomic hybridization. Proc Natl Acad Sci USA 91:2156–2160 (1994).

Kallioniemi OP, Kallioniemi A, Sudar D, Rutovitz D, Gray JW, et al: Comparative genomic hybridization: a rapid new method for detecting and mapping DNA amplification in tumors. Semin Cancer Biol 4:41–46 (1993).

Kallioniemi OP, Kallioniemi A, Piper J, Isola J, Waldman FM, et al: Optimizing comparative genomic hybridization for analysis of DNA sequence copy number changes in solid tumors. Genes Chromosomes Cancer 10:231–243 (1994).
Kirchhoff M, Gerdes T, Rose H, Maahr J, Ottesen AM, Lundsteen C: Detection of chromosomal gains and losses in comparative genomic hybridization analysis based on standard reference intervals. Cytometry 31:163–173 (1998).
Kirchhoff M, Gerdes T, Maahr J, Rose H, Bentz M, et al: Deletions below 10 megabasepairs are detected in comparative genomic hybridization by standard reference intervals. Genes Chromosomes Cancer 25:410–413 (1999).
Kirchhoff M, Rose H, Lundsteen C: High resolution comparative genomic hybridisation in clinical cytogenetics. J Med Genet 38:740–744 (2001).
Knight SJ, Flint J: Perfect endings: a review of subtelomeric probes and their use in clinical diagnosis. J Med Genet 37:401–409 (2000).
Kowalska A, Bozsaky E, Ramsauer T, Rieder D, Bindea G, et al: A new platform linking chromosomal and sequence information. Chromosome Res 15:327–339 (2007).
Lichter P, Bentz M, Joos S: Detection of chromosomal aberrations by means of molecular cytogenetics: painting of chromosomes and chromosomal subregions and comparative genomic hybridization. Methods Enzymol 254:334–359 (1995).
Lichter P, Joos S, Bentz M, Lampel S: Comparative genomic hybridization: uses and limitations. Semin Hematol 37:348–357 (2000).
Lin KW, Yan J: The telomere length dynamic and methods of its assessment. J Cell Mol Med 9: 977–989 (2005).
Narath R, Ambros IM, Kowalska A, Bozsaky E, Boukamp P, Ambros PF: Induction of senescence in *MYCN* amplified neuroblastoma cell lines by hydroxyurea. Genes Chromosomes Cancer 46:130–142 (2007).
Pinkel D, Segraves R, Sudar D, Clark S, Poole I, et al: High resolution analysis of DNA copy number variation using comparative genomic hybridization to microarrays. Nat Genet 20:207–211 (1998).
Piper J, Rutovitz D, Sudar D, Kallioniemi A, Kallioniemi OP, et al: Computer image analysis of comparative genomic hybridization. Cytometry 19:10–26 (1995).
Riethman H, Ambrosini A, Paul S: Human subtelomere structure and variation. Chromosome Res 13:505–515 (2005).
Schweizer D: Reverse fluorescent chromosome banding with chromomycin and DAPI. Chromosoma 58:307–324 (1976).
Schweizer D: Counterstain-enhanced chromosome banding. Hum Genet 57:1–14 (1981).
Schweizer D, Ambros PF: Chromosome banding. Stain combinations for specific regions. Methods Mol Biol 29:97–112 (1994).
Selzer RR, Richmond TA, Pofahl NJ, Green RD, Eis PS, et al: Analysis of chromosome breakpoints in neuroblastoma at sub-kilobase resolution using fine-tiling oligonucleotide array CGH. Genes Chromosomes Cancer 44:305–319 (2005).
Stock C, Kager L, Fink FM, Gadner H, Ambros PF: Chromosomal regions involved in the pathogenesis of osteosarcomas. Genes Chromosomes Cancer 28:329–336 (2000).
Wang N: Methodologies in cancer cytogenetics and molecular cytogenetics. Am J Med Genet 115: 118–124 (2002).